ACS OMEGA

Open Access

http://pubs.acs.org/journal/acsodf

Article

Antimicrobial Activities of *Pistacia lentiscus* Essential Oils Nanoencapsulated into Hydroxypropyl-beta-cyclodextrins

Obaydah Abd Alkader Alabrahim and Hassan Mohamed El-Said Azzazy*

Cite This: *ACS Omega* 2024, 9, 12622−12634

Read Online

ACCESS | Metrics & More | Article Recommendations | Supporting Information

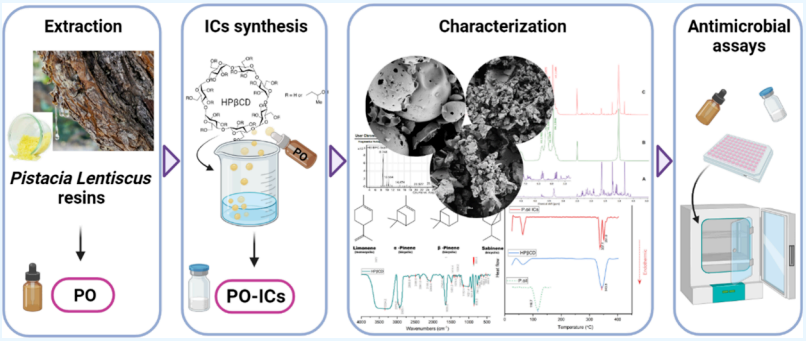

ABSTRACT: The rising risks of food microbial contamination and foodborne pathogens resistance have prompted an increasing interest in natural antimicrobials as promising alternatives to synthetic antimicrobials. Essential oils (EOs) obtained from natural sources have shown promising anticancer, antimicrobial, and antioxidant activities. EOs extracted from the resins of *Pistacia lentiscus* var. *Chia* are widely utilized for the treatment of skin inflammations, gastrointestinal disorders, respiratory infections, wound healing, and cancers. The therapeutic benefits of *P. lentiscus*essential oils (PO) are limited by their low solubility, poor bioavailability, and high volatility. Nanoencapsulation of PO can improve their physicochemical properties and consequently their therapeutic efficacy while overcoming their undesirable side effects. Hence, PO was extracted from the resins of *P. lentiscus*via hydrodistillation. Then, PO was encapsulated into (2-hydroxypropyl)-beta-cyclodextrin (HPβCD) via freeze-drying. The obtained inclusion complexes (PO-ICs) appeared as round vesicles (22.62 to 63.19 nm) forming several agglomerations (180 to 350 nm), as detected by UHR-TEM, with remarkable entrapment efficiency (89.59 ± 1.47%) and a PDI of 0.1475 ± 0.0005. Furthermore, the encapsulation and stability of PO-ICs were confirmed via FE-SEM, ^{1}H NMR, 2D HNMR (NOESY), FT-IR, UHR-TEM, and DSC. DSC revealed a higher thermal stability of the PO-ICs, reaching 351.0 °C. PO-ICs exerted substantial antibacterial activity against *Pseudomonas aeruginosa*, *Staphylococcus aureus*, and *Escherichia coli* as compared to free PO. PO-ICs showed significant enhancement in the antibacterial activity of the encapsulated PO against *S. aureus* with an MIC90 of 2.84 mg/mL and against *P. aeruginosa* with MIC90 of 3.62 mg/mL and MIC50 of 0.56 mg/mL. In addition, PO-ICs showed greater antimicrobial activity against *E. coli* by 6-fold with an MIC90 of 0.89 mg/mL, compared to free PO, which showed an MIC90 of 5.38 mg/mL. In conclusion, the encapsulation of PO into HPβCD enhanced its aqueous solubility, stability, and penetration ability, resulting in a significantly higher antibacterial activity.

1. INTRODUCTION

The rising risks of food microbial contamination and foodborne pathogens resistance have prompted an increasing interest in natural antimicrobials as promising alternatives to synthetic antimicrobials.[1−3] Essential oils (EOs), in particular, have been considered as promising antimicrobial agents for controlling foodborne pathogens and microbial growth, owing to their rich content of various bioactive compounds and their intrinsic antimicrobial activities.[1−9] For instance, the EOs of rosemary, sage, and citrus have been used as food preservatives and available commercially in Spain in the "DMC Base Natural" product.[7] Another example is the use of carvone, derived from the EOs extracted from the caraway seed, as an antifungal fighter and a sprout inhibitor for potatoes and is also available commercially in The Netherlands in the "Talent" product.[9] Additionally, EOs extracted from the tea tree (*Melaleuca alternifolia*) have been commercially utilized as antiseptics.[6]

Many EOs have been employed by different industries in the European Union, including their use in perfumes, pharmaceutical products, and food flavorings and additives.[4,5] Additionally, most EOs have been recognized as *Generally*

Received: September 25, 2023
Revised: January 5, 2024
Accepted: January 11, 2024
Published: March 4, 2024

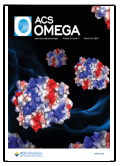

Recognized as Safe (GRAS), provoking their advantageous use as food preservatives and additives.[10,11]

Pistacia lentiscus var. *Chia* belongs to the Anacardiaceae family, which involves at least 11 distinguished species. The fruits, resins, and aerial parts of these species were extensively investigated, and their extracts have been widely utilized for wound healing, tumor targeting, and treatment of skin inflammation, gastrointestinal disorders, and respiratory infections.[12−20] Additionally, owing to their distinguished therapeutic properties, the EOs extracted from the resins of *P. lentiscus* var. *Chia* (PO) have been broadly exploited in the medicinal, pharmaceutical, food, and cosmetic industries.[21] Furthermore, the European Committee on Herbal Products (HMPC) approved the use of *P. lentiscus* resins as a natural medicine in 2015.[21] Previous *in vivo* studies and clinical trials have shown an effective antibacterial activity of *P. lentiscus* resins, particularly against *Helicobacter pylori,* a main cause of gastric ulcers and gastric cancers, in.[22−26] Since 1995, additional antimicrobial activities exerted by *P. lentiscus* extracts have been reported against different Gram+ve and Gram-ve bacteria, including *Salmonella enteritidis*, *Pseudomonas fragi*, *Lactobacillus plantarum*, *Staphylococcus aureus*, *Escherichia coli*, *Pseudomonas aeruginosa*, and different *Streptococcus* species.[27−34]

The promising therapeutic properties of PO are attributed to their huge content of diverse bioactive compounds such as triterpenes, monoterpenoids, oxygenated terpenes, nonoxygenated terpenes, and polyphenols. Hence, PO have been considered as promising antioxidants, anti-inflammatory agents, antimicrobials, and anticancers.[12−20] However, the ultimate benefits of PO for clinical applications have been hindered by their low solubility, poor bioavailability, reduced stability, and high volatility. Therefore, several nanocarriers were exploited to encapsulate and maximize the biological activities of PO.[35−38]

Cyclodextrins represent a group of cyclic oligosaccharides comprising several glucopyranosyl units linked by α-(1,4) bonds. Also, the most common types of cyclodextrins utilized are α-, β-, and γ-cyclodextrins, which are structurally distinguished by the number of glucopyranose units, entailing six, seven, or eight glucopyranose units in their structures, respectively.[39,40] Also, the use of these three cyclodextrins as food additives has been approved by the Food and Drug Administration (FDA), and they are further recognized as GRAS.[41,42] More importantly, the distinguished structure of cyclodextrins, consisting of a hydrophobic cavity and a hydrophilic surface, facilitates the formation of different inclusion complexes (ICs) with various guests and molecules, enhancing their physicochemical properties, solubility, stability, release sustainability, and bioavailability resulting in superior therapeutic activity.[40,43] Hydroxypropyl-beta-cyclodextrins (HPβCD) refer to the simple structures of β-cyclodextrins attached with hydroxypropyl groups to their surfaces, resulting in higher water solubility and better safety profiles.[44] Moreover, the intravenous and oral use of HPβCD and the topical application of 2-hydroxypropyl-γ-cyclodextrins have been approved by the FDA as additives/excipients.[45,46]

EOs encapsulation into cyclodextrins and their derivatives have shown several positive outcomes, including superior stability, extended shelf life storage duration, increased solubility and bioavailability, sustained release capability, and higher therapeutic and antimicrobial activities of the encapsulated EOs.[47−52] Several studies reported the successful encapsulation of different EOs into cyclodextrins, showing more significant antimicrobial activities.[47,52−54] For instance, the EOs of black pepper showed higher antibacterial activities against *S. aureus* and *E. coli* by two- to four-fold upon their encapsulation into HPβCD.[53] Also, the EOs of carvacrol, star anise, thymol, and thyme showed higher antimicrobial activities upon their encapsulation into HPβCD.[47,52,54]

Thus, the current work aimed to extract PO from *P. lentiscus* var. *Chia* resins using a green extraction method of hydrodistillation and prepare their ICs with HPβCD (PO-ICs) via a freeze-drying method. Also, the physicochemical properties of the obtained PO-ICs were investigated in addition to their antibacterial activities against *S. aureus*, *E. coli*, and *P. aeruginosa*. *E. coli* and *S. aureus* are two common types of bacteria that cause foodborne illnesses and food contamination.[55] Although *P. aeruginosa* has scarcely been linked to food-borne pathogens, it is recognized as an opportunistic bacterium. Also, *P. aeruginosa* was isolated from drinking water, food, soil, salads, and vegetables and could cause serious infections.[56] This bacterium can further colonize, forming biofilms on surfaces, making their targeting by conventional antiseptics and disinfectants even more challenging.[57] Because of the unique properties of cyclodextrins (FDA-approved for use as food additives and excipients), they have been used for encapsulation of several bioactive components including EOs, which might encourage their promising use in food-packaging and preservatives for controlling microbial growth and contamination.

2. MATERIALS AND METHODS

2.1. Microorganisms. The bacteria strains of *Staphylococcus aureus*, *Escherichia coli*, and *Pseudomonas aeruginosa* (ATCC numbers 25923, 25922, and 27853, respectively) were purchased from Nawah Scientific Inc., Cairo, Egypt. Bacteria were cultivated in nutrient broth and incubated for 24 h at 37 °C. All bacteria were preserved at −20 °C in glycerol (15% v/v).

2.2. Chemicals. HPβCD were purchased from Sigma (Sigma-Aldrich, Germany). Acetonitrile (HPLC and UV grade) was obtained from VWR BDH Chemicals (Fontenay-sous-Bois, France). KBr (FT-IR grade) was purchased from Merck (KGaA, Darmstadt, Germany). Dimethyl sulfoxide (DMSO) was provided by Fisher Scientific (Loughborough, UK). Other reagents were of analytical grade. Natural Chios mastic gums (small tears), *P. lentiscus* variety *Chia*, were provided by the Chios Gum Mastic Growers Association, Chios, Greece.

2.3. Green Extraction of EOs from the Resins of the *P. lentiscus* variety *Chia*. Following the European pharmacopeia monograph of Mastic (01/2008:1876),[58,59] a hydrodistillation extraction process was applied to extract the EOs from the resins of *P. lentiscus* variety *Chia*, using a Clevenger apparatus. Briefly, the small yellowish resins (gums) of the *P. lentiscus* variety *Chia* had been initially transformed into a fine aromatic white powder employing a lab mortar. Afterward, 30 g of the obtained powder was added to 300 mL of distilled water in a 500 mL round-bottomed flask, placed into a heating mantle, for which a constant heat supply could be provided, reaching a steady boiling point at 95 to 105 °C. Subsequently, the steam that carries PO was condensed, providing two distinguished layers of water and PO. The process continued for at least 3 h, where each 30 g of powder required 3 h of extraction. This process was repeated using several batches,

https://doi.org/10.1021/acsomega.3c07413
ACS Omega 2024, 9, 12622−12634

reaching a total of 5 g of PO collected out of 500 g of *P. lentiscus* resins. PO was then gathered and collected in one dark and well-sealed amber glass and stored at 4 °C. Hence, the final yield was 1% (w/w). At the end of the extraction processes, all of the characterization, analyses, and antimicrobial assays were performed on the collected PO. Notably, the obtained PO had low viscosity, unique aroma, and yellow color.

2.4. PO Compositional Analysis (GC-MS analysis). GC-MS analysis was performed to analyze the components of the PO obtained. For this purpose, Agilent Technologies gas chromatography (7890B) and mass spectrometer detector (5977B) were utilized following previous reports.[60]

2.5. Encapsulation of PO into HPβCD. The encapsulation of PO into HPβCD was accomplished via the formation of their ICs employing the freeze-drying method.[54,61] For this purpose, 500 mg of PO was dispersed in an aqueous solution of HPβCD, in which 5 g of HPβCD was dissolved in 25 mL of distilled water.[53,62] The obtained mixture was then kept in a sealed container and left on a stirrer (200 rpm) for 24 h at room temperature while being protected from light to allow the formation of PO-ICs. After that, the resulting suspension was filtered through 0.45 μm PTFE filters to eliminate unencapsulated particles. Consequently, the obtained solution, which now contains PO-ICs only, was left in a freezer (−20 °C) for 16 h and was then lyophilized until all moisture got sublimated (approximately 48 h), using a freeze-dryer (TOPT-10C freeze-dryer, Toption Group Co., Limited, Xi'an, China). Lastly, the lyophilized powder obtained was stored in a sealed container and protected from light inside a desiccator until use.

2.6. Physicochemical Characterizations and Bioassays of PO and PO-ICs. *2.6.1. Particle Size and Polydispersity Index (PDI) Determination.* The average particle size and polydispersity indices of the free HPβCD and PO-ICs were determined using a Zetasizer Nano-ZS employing dynamic light scattering (Malvern Instruments Ltd., Malvern, UK). For this purpose, powder samples of HPβCD and PO-ICs were dispersed in distilled water in a 3:1 ratio (w/v). All measurements were conducted at 25 °C.[63]

2.6.2. Morphological Examination. The morphology of PO-ICs and free HPβCD was examined by utilizing a LEO Field Emission Scanning Electron Microscope (FE-SEM) (Leo Supra 55, Zeiss Inc., Oberkochen, Germany). Powder samples of PO-ICs and HPβCD were fixed on aluminum stubs and then coated with a thin layer of Au (10 mA for 8 min of Au sputtering) before their observation under 500× magnification.[62]

Furthermore, an ultrahigh-resolution transmission electron microscope (UHR-TEM; JEOL, JEM-2100 Plus, Tokyo, Japan) operating at an accelerating voltage of 200 kV was used to investigate the shapes of PO-ICs particles and to confirm the encapsulation of PO. Briefly, aqueous suspensions of free HPβCD and PO-ICs were prepared in distilled water and sonicated for 10 min (37 °C). A drop of each suspension was then placed directly onto a copper grid covered with carbon film (standard option A, 1 nm) followed by staining using a droplet of 2% uranyl acetate to improve the field contrast. Grids were allowed to dry at room temperature on filter papers before observation under two main times of magnifications of 5000 and 25000.[54]

2.6.3. Fourier Transform Infrared Spectroscopy (FT-IR) Examination of PO-ICs, HPβCD, and PO. FT-IR spectra of PO-ICs, free PO, and free HPβCD were detected in the spectral range of 4000−400 cm^{-1} to examine the chemical structures of the obtained compounds and to ensure the incorporation of PO into HPβCD (Nicolet 380 FT-IR, Thermo Scientific, Madison, WI). For the free PO sample, a small drop was spread on a piece of KBr window and placed directly in front of an IR beam. For PO-ICs and free HPβCD, tiny amounts were first mixed with KBr (FT-IR grade) at a 1:100 ratio, and the obtained mixtures could be compressed using a hydraulic press to form small discs (15T manual press machine, China).[64]

2.6.4. Entrapment Efficiency (%EE) and Drug loading (% DL) Capacity of PO-ICs. The amount of PO encapsulated into their ICs was calculated spectrophotometrically at 256 nm using a UV−vis double beam spectrophotometer (Cary 3500 UV−vis Engine, Agilent Technologies Australia (M) Pty Ltd., Mulgrave, Australia). First, 5 mg of PO-ICs was added to 5 mL of acetonitrile (99% HPLC- and UV-grade) in a sealed container protected from light. This solution was then left on an agitating shaker for 72 h at room temperature to allow enough time for the entrapped PO to be released from the PO-ICs and transferred to the solution (acetonitrile). After 72 h, the obtained solution contained the released PO in addition to the powder of the ICs (the leftover HPβCD) which precipitated at the bottom. Hence, few milliliters of the obtained solution, which contained the released PO, were withdrawn to be read spectrophotometrically. Under the same conditions, a standard curve for PO was prepared with a range of concentrations between 3.125 and 200 μg/mL (PO: $y = 0.0035x + 0.0161$, $r^2 = 0.9997$). The following equations (A) and (B) were used to calculate the %EE and %DL of PO-ICs, given that the EE was expressed as a w/w percentage of the PO amount entrapped into the ICs to the initial amount of the PO used for ICs formation:[54]

$$\%EE = \left[\frac{\text{amount of PO entrapped}}{\text{initial amount of PO utilized for ICs formation}}\right] \times 100$$

$$\%DL = \left[\frac{\text{amount of PO entrapped}}{\text{amount of ICs produced}}\right] \times 100$$

2.6.5. ^1H and 2D-NOESY NMR Spectra Analyses. The ^1H NMR spectra of HPβCD, PO, and PO-ICs as well as the 2D-NOESY spectrum of PO-ICs were investigated using an NMR spectrometer (BRUKER BioSpin GmbH, D-76287 Rheinstetten, Germany) at 25 °C and 400 MHz. For this purpose, samples were dissolved in DMSO and placed in an NMR tube.[47]

2.6.6. Thermal Stability Studies. Thermal behaviors and stabilities of the HPβCD, PO, PO-ICs, and PO-HPβCD physical mixture (1:10) were carried out using a differential scanning calorimeter (DSC-60 Plus model, Shimadzu Corp., Kyoto, Japan). Samples were accurately weighed and placed on an aluminum pan, and a heat flow was provided at a rate of 10 °C/min between 28 and 400 °C under an atmosphere of nitrogen.[54] Additionally, the melting points of *P. lentiscus* gum and its corresponding powder were determined using a Fisher-Johns Melting Point Apparatus (Fischer Scientific, Milton, DE). Briefly, the temperature at which the gum/powder started to melt was recorded, the final temperature at which the gum/powder showed complete melting was recorded, and the average temperatures were determined.

https://doi.org/10.1021/acsomega.3c07413
ACS Omega 2024, 9, 12622−12634

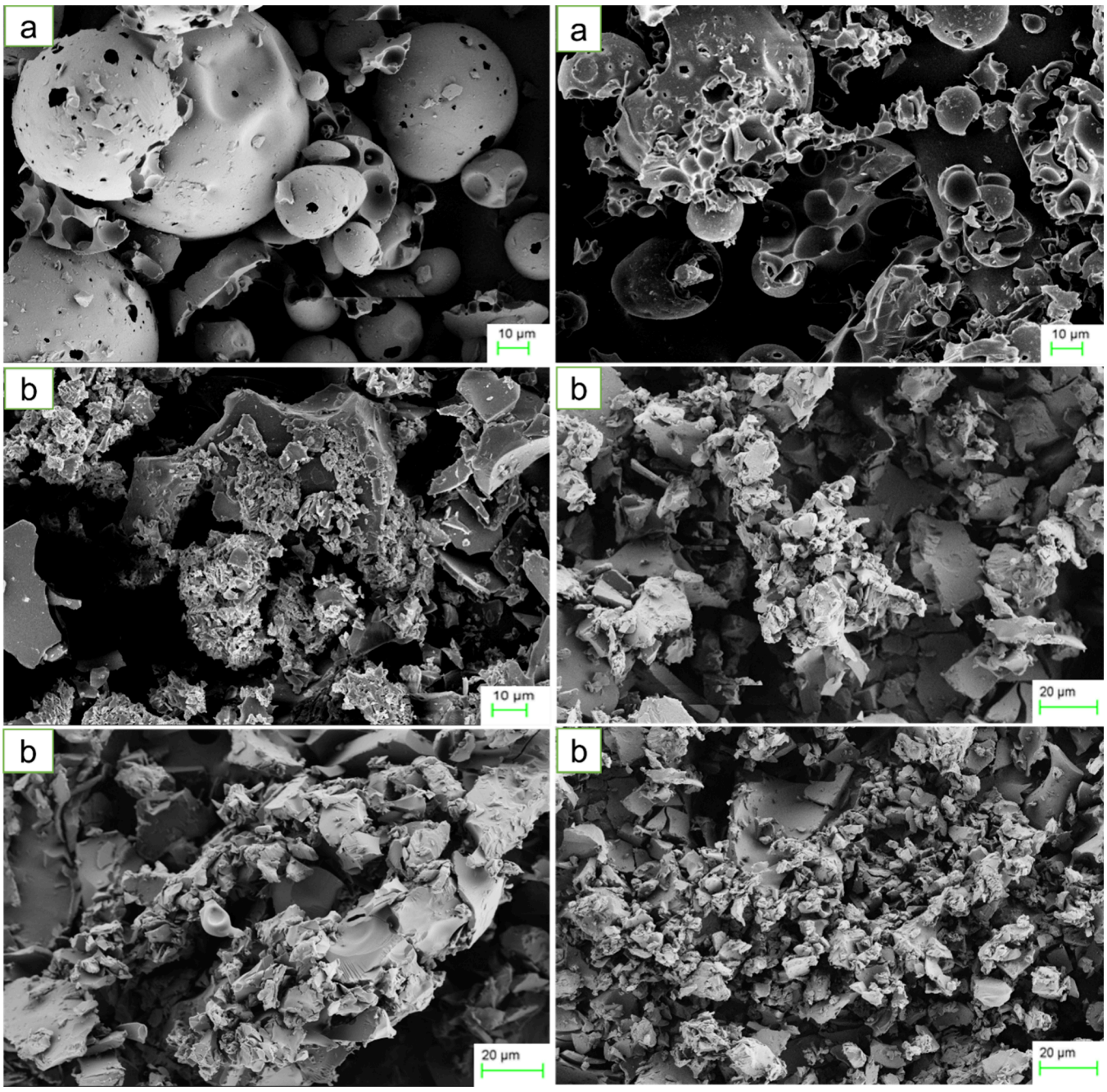

Figure 1. FE-SEM images of free HPβCD (a) and PO-ICs (b). HPβCD showed variable sizes of rectangular-shaped crystals and some intact ovoid-shaped particles. In contrast, PO-ICs exhibited many agglomerations and substantial changes in the particles' morphology with considerable size reduction. These changes indicate the successful establishment of the inclusion complexes.

2.6.7. Antimicrobial Activity Investigation. The antimicrobial activities of free HPβCD, PO, and PO-ICs were examined against *P. aeruginosa*, *S. aureus*, and *E. coli* using a broth microdilution assay in 96-well microplates, as previously described with minor modifications.[47,53] For this purpose, the microbial suspensions of bacteria were prepared in 250 mL flasks and cultivated at 37 °C for 24 h. Then, the microbial suspensions were diluted to obtain 10^5 CFU/mL. Consequently, 10 μL of each microbial suspension was added to 90 μL of nutrient broth (Titan Biotech Ltd., Rajasthan, India), containing several concentrations of PO and PO-ICs. For free PO, the concentrations added were in the range of 0.34 to 5.4 mg/mL. For PO-ICs, the concentrations added were in the range of 0.25 to 4.09 mg/mL. The concentrations of the encapsulated PO were determined based on the encapsulation efficiency. Following their filtration using 0.20 μm syringe filters, PO-ICs were added to the plates as aqueous suspensions, whereas PO was added as aqueous micro-emulsions. Positive control wells were filled with microbial suspensions, whereas negative control wells were filled with PO or PO-ICs. The microplates were incubated in the dark for 24 h at 37 °C. Consequently, the turbidity reflected by optical density was read at 570 and 600 nm using a FLUOstar microplate reader (BMG Labtech, Ortenberg, Germany). MIC values of PO and PO-ICs were recorded and expressed by the lowest concentration that showed no visible growth in the

https://doi.org/10.1021/acsomega.3c07413
ACS Omega 2024, 9, 12622−12634

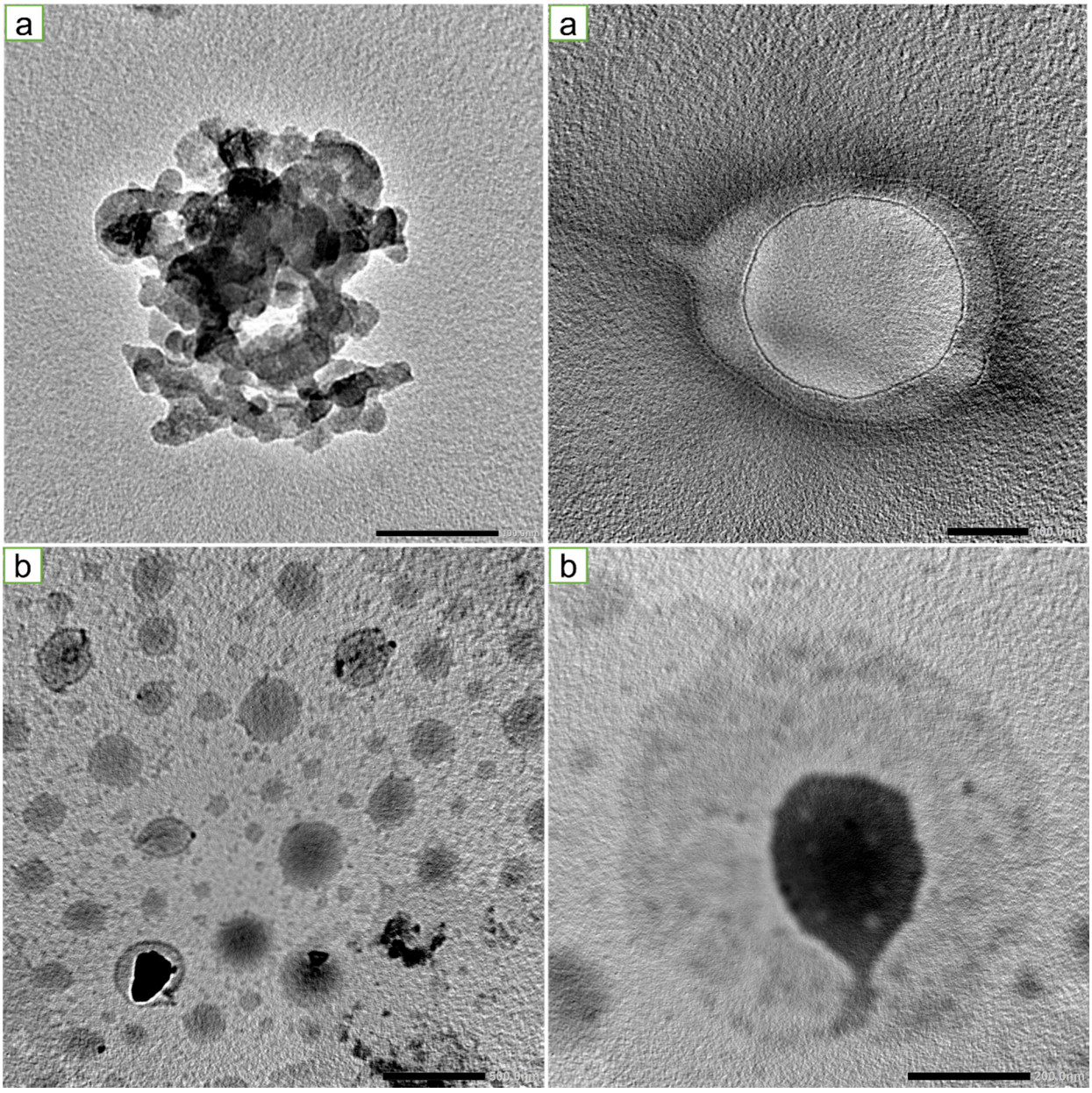

Figure 2. UHR-TEM images of free HPβCD (a) and PO-ICs (b), depicting the morphological and structural characteristics of free and encapsulated particles. PO-ICs can be seen with round (presumably spherical)-shaped vesicles. A thin membrane layer surrounding the PO could also be noticed. Some of the ICs were revealed with larger vesicles and irregular and hexagonal shapes. Additionally, particles exhibited clear evidence of agglomeration, where large particles attract smaller ones. On the other hand, free HPβCD showed round-shaped vesicles mostly forming self-assembled larger structures.

wells after 24 h of incubation.[47,53,65−67] Under the same conditions, ciprofloxacin was used as a positive control within a range of 10 to 0.001 μg/mL. All measurements were performed in triplicate.

2.7. Statistical Analysis. Data and results were reported as the mean ± standard deviation (SD). All formulations were prepared in triplicate. One-way analysis of variances was used to determine statistical differences, and a p value of $\leq$0.05 was considered to report statistically significant differences. GraphPad Prism 8.0.2, Spline-LOWESS, was used to determine MIC values of the antimicrobial assay.

3. RESULTS AND DISCUSSION

3.1. PO Analysis Using GC-MS. Twenty-nine compounds were identified by the GC-MS analysis performed on PO (Supporting Information Figure S1 and Table S1).[35] The mass spectrum was first compared to the NIST library, and the major components detected were α-pinene (81.20%), β-myrcene (4.70%), and β-pinene (2.97%), which belong to the monoterpenes group. Other chemical groups identified by GC-MS included oxygenated monoterpenes, phenylpropanoids, oxygenated sesquiterpenes, and sesquiterpenes. The GC-MS findings of PO came in agreement with previous reports.[58,68]

3.2. Particle Size and PDI Determination. The average diameter and PDI values of the PO-ICs were determined. The

https://doi.org/10.1021/acsomega.3c07413
ACS Omega 2024, 9, 12622−12634

PDI index can detect the uniformity of the particle sizes in a certain suspension. A PDI value greater than 0.7 indicates a highly polydisperse system, whereas a value of less than 0.08 refers to a nearly monodispersed system.[69] Also, agglomerations between the suspension particles can be indicated with PDI values greater than 0.07, whereas lower PDI values (<0.07) refer to very few agglomerations.[70] Free HPβCD showed an average particle size of 1.125 μm (1125.73 nm) and a highly heterogeneous and dispersed system with a PDI value of 0.801. Conversely, the PO-ICs suspension displayed greater stability with smaller particles and a less dispersed system. PO-ICs showed an average particle size of 368.5 ± 0.55 nm and a PDI of 0.1475 ± 0.0005. These findings might be explained by the high tendency of free HPβCD and ICs particles to agglomerate due to the cyclodextrin self-assembly in water.[54] Notably, the hydrophilic aggregates developed by cyclodextrins and their complexes can dissolve lipophilic compounds through complexation and/or micelle-like structures formation.[71] Current findings are further supported by similar results reported previously.[62,71−73]

3.3. Morphological Investigation. FE-SEM images of free HPβCD (Figure 1a) and PO-ICs (Figure 1b) present the morphological and size changes among the HPβCD and PO-ICs. HPβCD showed variable sizes of rectangular-shaped crystals and some intact ovoid-shaped particles. On the other hand, PO-ICs exhibited significant changes in the particles' morphology and crystals' shapes and sizes. The smaller particles and crystals of the PO-ICs compared to HPβCD support the results obtained by the Zetasizer. More importantly, PO-ICs showed several agglomerations in which large particles attract smaller particles. The aggregation of the smaller particles and their morphological transformations indicated the development of an amorphous product incorporating another compound in the complex, suggesting the successful establishment of the inclusion complexes. Similar results were reported previously.[54,72]

Furthermore, UHR-TEM images of free HPβCD (Figure 2a) and PO-ICs (Figure 2b) were obtained, depicting the morphological and structural characteristics of the free and encapsulated particles. PO-ICs were presented with presumably spherical shaped vesicles, with diameters ranging from 22.62 to 63.19 nm. A thin membrane layer surrounding the PO could also be noticed. Some of the PO-ICs were revealed with larger vesicles of irregular and hexagonal shapes. Additionally, particles exhibited clear evidence of several agglomerations with diameters of 180−350 nm, where large particles attract smaller ones. Nevertheless, PO encapsulation into HPβCD could hence be established. On the other hand, free HPβCD showed round shaped vesicles mostly forming self-assembled larger structures. The micellar structures observed in different shapes in both fields of free HPβCD and PO-ICs can be explained by the preparations of both samples in distilled water prior to their observations, in which free HPβCD and ICs particles have a high tendency to agglomerate due to the cyclodextrins self-assembly in water. Similar results supporting current findings were also reported.[54,63,74,75]

3.4. FT-IR Examination of HPβCD, PO, and PO-ICs. The FT-IR spectra of HPβCD, PO, and PO-ICs were investigated (Figure 3). The FT-IR spectrum of PO revealed absorption bands at 2919.0 cm^{-1} (methylene group stretching vibration), 2728.7 cm^{-1} (C−H stretching), 1681.1 cm^{-1} (H−O−H bending vibration), 1445.7 cm^{-1} (C−H scissoring vibration), 1369.2 cm^{-1} (C−O stretching vibration), 887.4 cm^{-1} (C−H bending of aromatic rings), 787.1 cm^{-1} (C−H bending), and 1270.0, 1200.1, and 1130.6 cm^{-1} (C−O−C stretching vibration). On the other hand, the FT-IR spectrum of HPβCD showed prominent bands of absorption at 3334.2 cm^{-1} (O−H stretching), 2970.6 cm^{-1} (=CH_2 symmetric stretching), 2925.1 cm^{-1} (methylene group stretching vibration), 1639.0 cm^{-1} (H−O−H bending vibration), 1481.3 cm^{-1} (C−H vibration), and 1021.4 and 1152.4 cm^{-1} for C−O−C symmetric and asymmetric stretching vibrations, respectively.

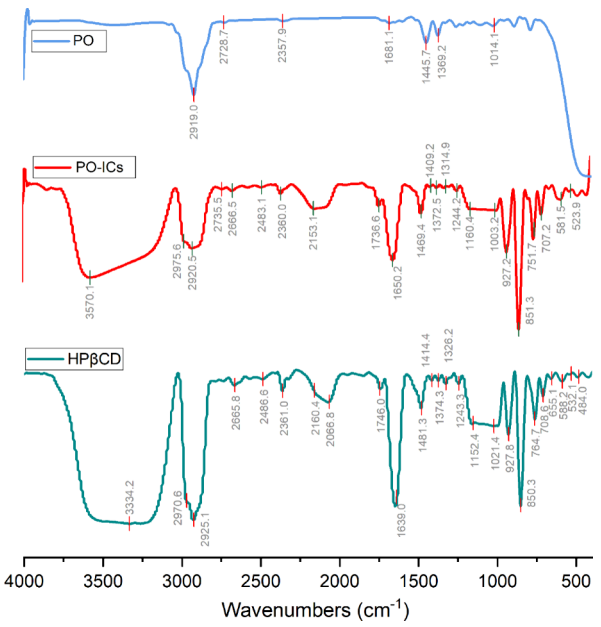

Figure 3. FT-IR spectra of free PO, PO-ICs, and HPβCD.

For the FT-IR spectrum of PO-ICs, all absorption bands of PO were masked by the intense bands of HPβCD, except for certain band shifts and the decrease in the broadening of the O−H band. This change in the O−H band might reflect the formation of some intermolecular hydrogen bonds between HPβCD and some PO components,[64] in which not only the encapsulation of these components inside the HPβCD cavity could happen but also interactions outside the HPβCD cavity might occur, as reported previously.[71] Additionally, the broader band of the methylene group (−CH_2) that appeared at 2920 cm^{-1} could suggest the successful entry of the PO's hydrophobic components into the HPβCD cavities.[64] Therefore, these findings indicate the successful encapsulation of PO into the HPβCD and the formation of stable inclusion complexes. Similar findings were previously reported.[47,62,64] It is worth noting that the stability of the main functional groups and chemical components of PO and PO-ICs were observed, where their corresponding FTIR spectra have been reinvestigated after 6 months. Interestingly, the same spectra were obtained, suggesting that the chemical composition of PO and PO-ICs was not changed.

3.5. Entrapment Efficiency (%EE) and Drug Loading (%DL) Capacity. The %EE and %DL of PO-ICs were determined with (89.59 ± 1.46)% and (9.09 ± 1.33)%, respectively. Interestingly, PO-ICs showed excellent entrapment efficiency, which might be explained by the prolonged complexation provided during the preparation process while keeping the complex solutions well protected and tightly sealed during both the preparation and drying steps. The influence of

https://doi.org/10.1021/acsomega.3c07413
ACS Omega 2024, 9, 12622−12634

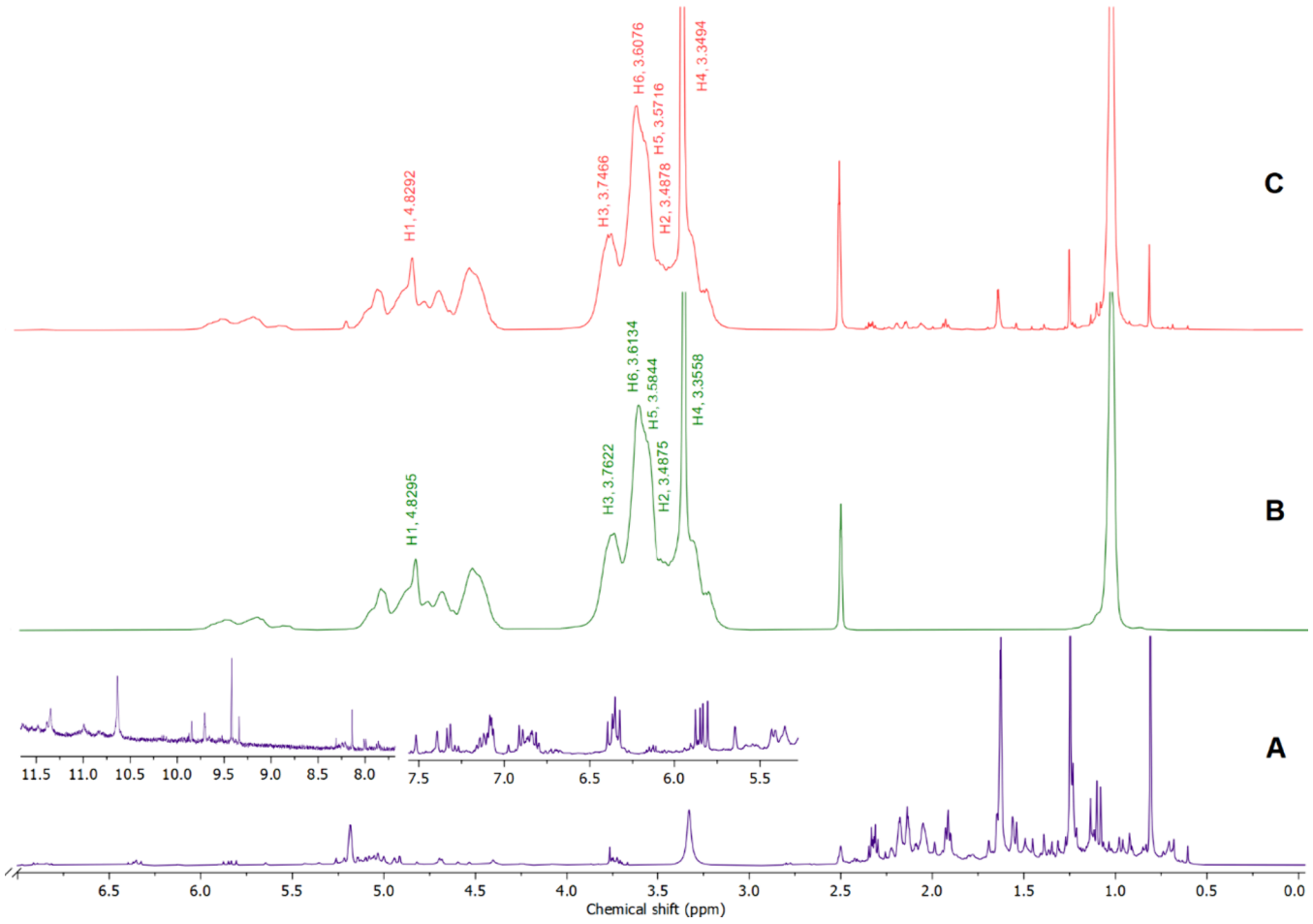

Figure 4. ^{1}H NMR spectra of PO (A), HPβCD (B), and PO-ICs (C).

the complexation time and drying steps on the percentage of EOs entrapment inside HPβCD was previously reported.[73] Also, some components shown by the GC-MS analysis of PO tend to have high affinities toward HPβCD such as α-pinene, limonene, and δ-3-carene.[53] Therefore, the excellent %EE of PO might be attributed to the high contents of α-pinene, limonene, and δ-3-carene components in PO (81.20, 0.77, and 1.11%, respectively). Additionally, these findings can be supported by the FT-IR analysis of the PO-ICs revealed above. On the other hand, the %DL results were satisfactory with 9.09% for PO-ICs, supporting previous studies.[54]

3.6. ^{1}H and 2D-NOESY NMR Spectra Analyses. ^{1}H NMR is used to investigate the spatial position and to confirm the encapsulation of a guest molecule inside the hydrophobic cavity of HPβCD and other cyclodextrins. The proton atoms located at positions 3 and 5 (H3 and H5) at the inner cavity of the HPβCD are shifted once a guest molecule enters the HPβCD cavity. The chemical shifts of H3 and H5 protons happen because of the interactions induced by the guest molecule(s) entering the hydrophobic cavity of HPβCD.[76]

The ^{1}H NMR spectra of PO, HPβCD, and PO-ICs are presented in Figure 4. PO's spectrum showed several proton peaks at 7.51, 7.39, 7.31, 7.09, 6.91, and 6.84 ppm, indicating that the molecular composition of PO contains aromatic structures. Also, the proton peaks appearing at 6.35 and 6.13 ppm confirm the presence of double bonds, whereas protons observed at 3.33, 3.67, and 3.77 ppm refer to the presence of C−O−C structures. Other characteristic proton peaks related to methylene or methyl structures linked to a double bond were shown at 1.91 and 1.78 ppm. Hence, these results confirm the analytical findings of the FT-IR and GC-MS analyses.

Furthermore, the ^{1}H NMR spectrum of the PO-IC spectrum (Figure 4) exhibited the proton peaks of both PO and HPβCD. Also, Figure 4B,C and Table 1 reveal the chemical shift changes of the protons linked to the D-glucopyranose units in the HPβCD molecules. Hence, there are five protons attached to the hydrophobic cavity of HPβCD. H1 is located in the middle of the structure of the HPβCD cavity. H2 and H4 are attached to the outside portion, whereas H6 is linked to the outermost side. While the H3 atom is located near the wider edge of the HPβCD cavity, the H5 atom can be revealed in the bottom side of the cavity. Moreover, the PO-IC spectrum showed negligible shifts in H1 and H2. Also, H4 and

Table 1. Chemical Shifts (δ) for HPβCD and PO-ICs and Differences in Chemical Shift ($\Delta\delta$)

proton	free HPβCD (δ/ppm)	PO-ICs (δ/ppm)	$\Delta\delta$ PO-ICs/free HPβCD ($\Delta\delta$/ppm)
H1	4.8295	4.8292	0.0003
H2	3.4875	3.4878	−0.0003
H3	3.7622	3.7466	0.0156
H4	3.3558	3.3494	0.0064
H5	3.5884	3.5716	0.0168
H6	3.6134	3.6076	0.0058

https://doi.org/10.1021/acsomega.3c07413
ACS Omega 2024, 9, 12622−12634

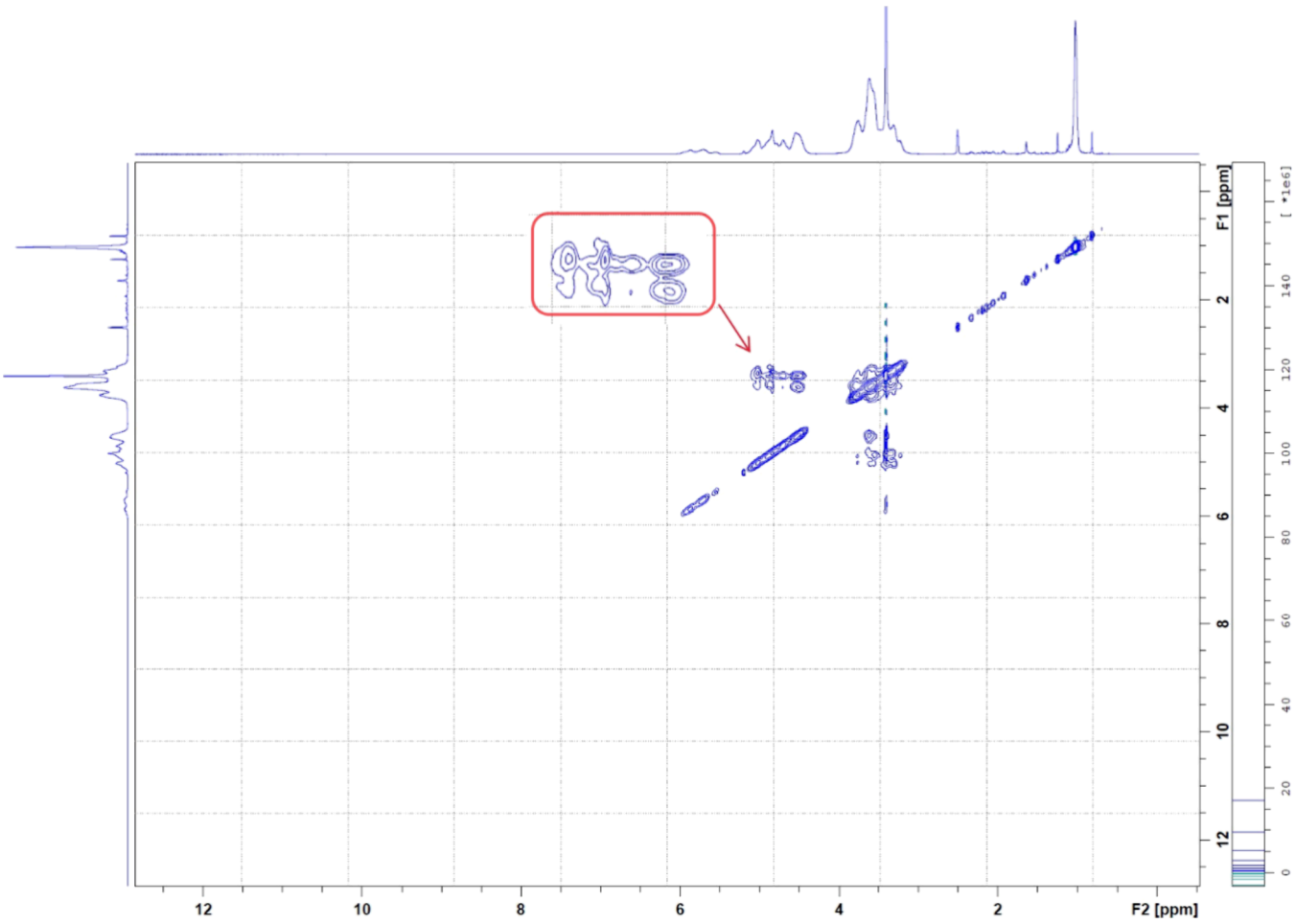

Figure 5. 2D-NOESY spectrum of PO-ICs in DMSO, demonstrating the interactions occurring between the PO protons and HPβCD protons inside the PO-ICs.

H6 were slightly shifted upfield, whereas H3 and H5 exhibited much stronger shifts upfield. These results suggest the successful entry of the aromatic and double bond structures of PO into the hydrophobic cavity of the HPβCD. In fact, the prominent upfield shifts noticed with H3 and H5 protons can be explained by the greater electron cloud densities developed. These higher densities might have been provoked by the prominent shielding effects of the aromatic structures and the double bonds shown in PO's compounds. These findings suggest the successful formation of PO-ICs.

Moreover, to further explore the inclusion mechanisms revealed by the entry of the PO into the hydrophobic cavity of HPβCD, 2D-NOESY NMR (nuclear Overhauser effect spectroscopy) was performed on PO-ICs. Such a technique observes the cross correlations that could originate from the spatial proximity established between the host (HPβCD) and the guest (PO components). The phenomenon of the nuclear Overhauser effect (NOE) could best describe the ICs formation, revealed by NMR spectroscopy, and can be translated by the transfer of the spin polarization from a single population (HPβCD) to another one (PO) happening among atoms in close proximity. Hence, the NOE cross correlation, crossed peaks, can be observed in a NOESY spectrum by the interaction presented by any two protons located near each other in the space (within 0.4 nm).[77,78] The 2D-NOESY spectrum of the PO-ICs obtained (Figure 5) depicted a considerable correlation, spatial proximity, between HPβCD protons (H3 and H5) and PO protons, supporting the chemical shifts revealed above, which eventually refer to the positive establishment of the PO-ICs and particularly the successful encapsulation of PO components into HPβCD cavities. Similar findings were shown by Saha et al.,[79] Rodríguez-López et al.,[80] and Khan et al.,[81] in which they could successfully report the effective encapsulation of different molecules into the cavities of HPβCD performing 2D-NMR spectroscopy, which showed similar positive correlations between the protons of the investigated molecules and the protons of the HPβCD (H3 and H5).[79−81]

3.7. Thermal Stability Studies. The physical characteristics of the obtained PO (i.e., color, aroma, and viscosity) were closely observed within 1 year of their extraction. PO was stored at 4 °C and protected from light in a tightly sealed amber glass. Within an entire year of observation, all the unique characteristics mentioned above were the same, indicating a very stable profile of the PO extracted.

The melting point of *P. lentiscus* gum was 130 °C, whereas its corresponding powder showed a melting point of 118 °C. On the other hand, DSC curves of the PO, HPβCD, PO-ICs, and PO-HPβCD physical mixture were obtained and investigated to confirm the PO-ICs formation and to examine their thermal behaviors and stabilities. In fact, the successful formation of PO-ICs can be confirmed by the shifting or vanishing of the endothermic melting peak associated with PO

https://doi.org/10.1021/acsomega.3c07413
ACS Omega 2024, 9, 12622−12634

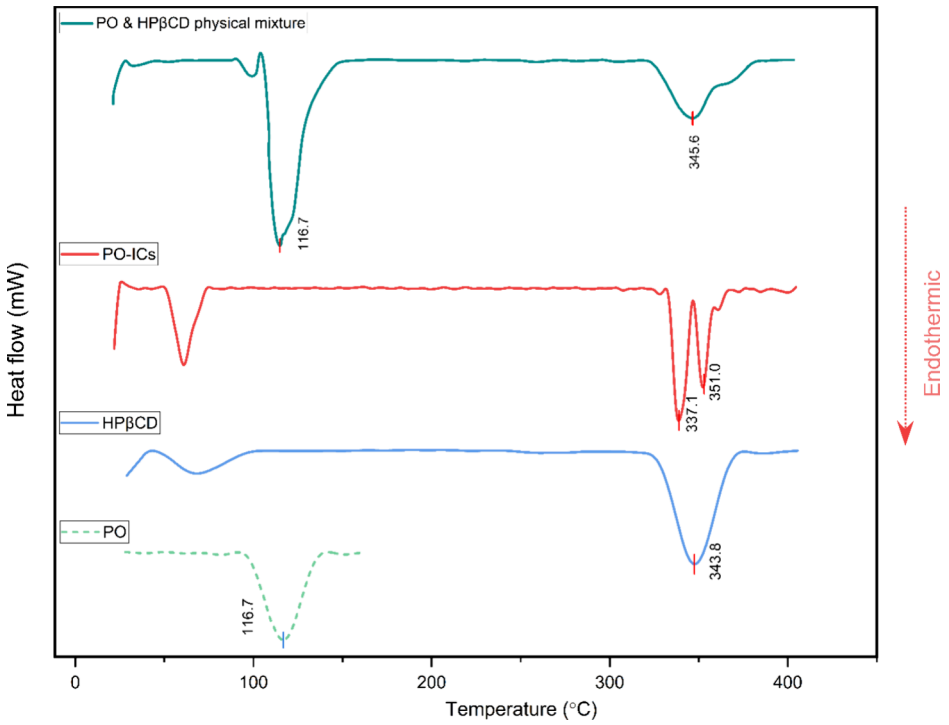

Figure 6. DSC thermograms of the PO, HPβCD, PO-ICs, and PO-HPβCD physical mixture.

Table 2. MIC Values of Free PO and PO-ICs Determined against *P. aeruginosa*, *E. coli*, and *S. aureus* Bacteria[a]

	P. aeruginosa			*E. coli*			*S. aureus*		
	MIC95	MIC90	MIC50	MIC95	MIC90	MIC50	MIC95	MIC90	MIC50
PO	>5.4 mg/mL	>5.4 mg/mL	5.33 mg/mL	>5.4 mg/mL	5.38 mg/mL	4.99 mg/mL	>5.4 mg/mL	>5.4 mg/mL	5.08 mg/mL
PO-ICs*	>4.09 mg/mL	3.62 mg/mL	0.56 mg/mL	3.6 mg/mL	0.89 mg/mL	<0.25 mg/mL	>4.09 mg/mL	2.84 mg/mL	0.54 mg/mL
Ciprofloxacin	0.13 μg/mL	0.12 μg/mL	0.06 μg/mL	0.14 μg/mL	0.12 μg/mL	0.02 μg/mL	0.14 μg/mL	0.13 μg/mL	0.06 μg/mL

[a]Spline-LOWESS, Graph-prism software, was used to calculate significant MIC values ($p < 0.05$) within the range of concentrations tested (5.4 to 0.34 mg/mL) for free PO, (4.09 to 0.25 mg/mL) for PO-ICs, and (10 to 0.001 μg/mL) for ciprofloxacin. * Values were calculated based on the entrapment efficiency.

on a DSC thermogram, indicating that PO is successfully entrapped into HPβCD.[54,82]

Figure 6 shows the DSC thermograms of the PO, free HPβCD, PO-ICs, and PO-HPβCD physical mixture. The HPβCD thermogram showed two endothermic peaks, one sharp peak observed at 343.8 °C, denoting the HPβCD melting, and a second peak shown below 100 °C, which refers to the evaporation of the water molecules. The PO thermogram showed one sharp endothermic peak at 116.7 °C associated with the PO's boiling point.

Moreover, the PO-ICs thermogram depicted three endothermic peaks. The first one was revealed at around 80 °C, denoting the presence of water molecules. The other two peaks were observed at 337.1 and 351.0 °C, indicating that an initial melting process of the HPβCD happened (at 337.1 °C) followed by a rapid boiling of the PO released from PO-ICs (at 351.0 °C). More importantly, the disappearance of the sharp endothermic peak, revealed by the PO thermogram at 116.7 °C, may refer to the encapsulation of the PO molecules in the HPβCD cavity. Also, the thermogram of the PO-HPβCD physical mixture could successfully show the melting peaks of PO and HPβCD at 116.7 and 345.6 °C, respectively, indicating positive establishment of the PO-ICs. In summary, the thermostable HPβCD molecules began to melt around 325 °C. This melting process induced the release of the thermolabile molecules of PO from the cavities of the HPβCD molecules. Consequently, the released PO components were exposed to extreme temperatures, resulting in their rapid boiling. These observations support the formation of PO-ICs and their greater thermal stability compared to free PO, which is in accordance with previous reports.[54,61,82,83] It is worth noting that the DSC study of the physical mixture of PO and HPβCD has been conducted after 3 months of their preparation, which could additionally refer to thermal stability of PO, where the same boiling point of PO was reported.

3.8. Antimicrobial Activity Investigation. The antimicrobial activities of ciprofloxacin, free HPβCD, free PO, and PO-ICs were investigated against *P. aeruginosa*, *E. coli*, and *S. aureus* bacteria. Table 2 exhibits the MIC values of PO, PO-ICs, and ciprofloxacin.

Ciprofloxacin is an effective bactericidal antibiotic belonging to the fluoroquinolone group (second generation) and has further shown reasonable bioavailability and bearable profile of side effects coupled with a potent activity exerted against Gram-negative and Gram-positive bacteria.[84]

The antimicrobial activity of PO can be attributed to their rich composition of monoterpenes and oxygenated monoterpenes, such as β-pinene, limonene, carvacrol, α-pinene, and thymol, which were reported to target the cellular membranes of the microbial cells and increase their permeability.[62,85−87]

https://doi.org/10.1021/acsomega.3c07413
ACS Omega 2024, 9, 12622−12634

Furthermore, the lipophilic nature of terpenes and their derivatives could facilitate their insertion and interruption of the lipid bilayers, hence increasing the cell membrane permeability, disturbing the cellular transport processes, and ultimately causing the death of bacteria.[85]

Free HPβCD (>100 mg/mL) failed to show any antimicrobial activities against the investigated bacteria. Furthermore, PO could not reveal significant antibacterial activity against *P. aeruginosa* within the range of the concentrations tested, except for an MIC50 value of 5.33 mg/mL. However, PO-ICs showed substantial enhancement of the encapsulated PO antibacterial activity against *P. aeruginosa* with MIC90 of 3.62 mg/mL and MIC50 of 0.56 mg/mL. In addition, PO-ICs showed an increase in PO activity against *E. coli* by 6-fold with an MIC90 of 0.89 mg/mL, compared to free PO which showed an MIC90 of 5.38 mg/mL. Also, PO-ICs revealed a greater activity against *S. aureus* with an MIC90 of 2.84 mg/mL, compared to free PO which failed to reveal an MIC90 value within the range of concentrations tested.

These results support the significance of encapsulating PO into HPβCD in enhancing their aqueous solubility, stability, and penetration ability, resulting in higher antimicrobial activities. In fact, EOs were reported to exert their antimicrobial activities inside the bacterial cytoplasm (protoplasm) and at their cell membranes. Hence, PO encapsulation into HPβCD might have facilitated their access to these sites by enhancing their aqueous solubility.[63,88]

4. CONCLUSIONS

EOs obtained from natural sources have shown promising anticancer, antimicrobial, and antioxidant activities. PO has been widely utilized for treating skin inflammations, gastrointestinal disorders, respiratory infections, wound healing, and cancers owing to its rich content of different bioactive compounds. In this work, PO was first extracted using the hydrodistillation extraction method and its chemical composition was analyzed using GC-MS analysis. Consequently, PO was encapsulated into HPβCD utilizing the freeze-drying method, and the obtained PO-ICs were investigated for their physicochemical properties. PO-ICs showed round vesicles (22.62 to 63.19 nm) forming several agglomerations (180 to 350 nm), as detetected by UHR-TEM, with remarkable %EE (89.59 ± 1.47%) and a PDI of 0.1475 ± 0.0005. ^{1}H NMR, 2D-NMR NOESY, DSC, UHR-TEM, FE-SEM, and FT-IR characterization tests confirmed the successful encapsulation and the stability of PO-ICs. Also, DSC results supported the successful encapsulation of PO and the higher thermal stability upon encapsulation into HPβCD. Eventually, PO-ICs showed greater and more significant antibacterial activities compared to free PO against *P. aeruginosa*, *S. aureus*, and *E. coli*. Hence, the encapsulation of PO into HPβCD showed remarkable enhancements of the PO stability profile and antimicrobial activity. These findings encourage the promising use of similar ICs for controlling food microbial-growth and contamination and for other therapeutic and cosmetic applications.

ASSOCIATED CONTENT

Supporting Information

The Supporting Information is available free of charge at https://pubs.acs.org/doi/10.1021/acsomega.3c07413.

GC-MS chromatogram of PO; PO compositional analysis (PDF)

AUTHOR INFORMATION

Corresponding Author

Hassan Mohamed El-Said Azzazy − *Department of Chemistry, School of Sciences & Engineering, The American University in Cairo, New Cairo 11835, Egypt; Department of Nanobiophotonics, Leibniz Institute of Photonic Technology, Jena 07745, Germany;* orcid.org/0000-0003-2047-4222; Phone: + 2 02 2615 2559; Email: hazzazy@aucegypt.edu

Author

Obaydah Abd Alkader Alabrahim − *Department of Chemistry, School of Sciences & Engineering, The American University in Cairo, New Cairo 11835, Egypt;* orcid.org/0000-0003-0906-7597

Complete contact information is available at: https://pubs.acs.org/10.1021/acsomega.3c07413

Notes

The authors declare no competing financial interest.

ACKNOWLEDGMENTS

This study was funded by a grant from the American University in Cairo to Prof. Hassan Azzazy.

LIST OF ABBREVIATIONS:

%DLbreakdrug loading capacity
%EEbreakentrapment efficiency
CFU/mLbreakcolony-forming unit per milliliter
DMSObreakdimethyl sulfoxide
DSCbreakdifferential scanning calorimetry
E. colibreak*Escherichia coli*
EOsbreakessential oils
FDAbreakFood and Drug Administration
FE-SEMbreakfield emission scanning electron microscope
FT-IRbreakFourier transform infrared spectroscopy
H. Pyloribreak*Helicobacter pylori*
HMPCbreakEuropean Committee on Herbal Products
HPβCDbreakhydroxypropyl-beta-cyclodextrins
ICsbreakinclusion complexes
IR beambreakinfrared beam
KBrbreakpotassium bromide
MICbreakminimum inhibitory concentration
NOEbreaknuclear Overhauser effect
NOESYbreaknuclear Overhauser effect spectroscopy
P. aeruginosabreak*Pseudomonas aeruginosa*
PDIbreakpolydispersity index
PObreak*Pistacia lentiscus* variety *Chia* essential oils
PO-ICsbreakinclusion complexes of the essential oils of *Pistacia lentiscus* variety *Chia* with hydroxypropyl-beta-cyclodextrins
S. aureusbreak*Staphylococcus aureus*

REFERENCES

(1) Alencar Filho, J. M. T. D.; Araújo, L. d. C.; Oliveira, A. P.; Guimarães, A. L.; Pacheco, A. G. M.; Silva, F. S.; Cavalcanti, L. S.; Lucchese, A. M.; Almeida, J. R. G. d. S.; Araújo, E. C. d. C. Chemical composition and antibacterial activity of essential oil from leaves of *Croton heliotropiifolius* in different seasons of the year. *Revista Brasileira de. Farmacognosia* **2017**, *27* (4), 440−444.

(2) El Hamdaoui, A.; Msanda, F.; Boubaker, H.; Leach, D.; Bombarda, I.; Vanloot, P.; El Aouad, N.; Abbad, A.; Boudyach, E. H.; Achemchem, F.; Elmoslih, A.; Ait Ben Aoumar, A.; El Mousadik, A. Essential oil composition, antioxidant and antibacterial activities of

wild and cultivated *Lavandula mairei Humbert*. *Biochemical Systematics and Ecology* **2018**, *76*, 1−7.
(3) Hąc-Wydro, K.; Flasiński, M.; Romańczuk, K. Essential oils as food eco-preservatives: Model system studies on the effect of temperature on limonene antibacterial activity. *Food Chem.* **2017**, *235*, 127−135.
(4) Burt, S. Essential oils: their antibacterial properties and potential applications in foods—a review. *Int. J. Food Microbiol.* **2004**, *94* (3), 223−253.
(5) Oosterhaven, K.; Poolman, B.; Smid, E. J. S-carvone as a natural potato sprout inhibiting, fungistatic and bacteristatic compound. *Industrial Crops and Products* **1995**, *4* (1), 23−31.
(6) Cox, S.; Mann, C.; Markham, J.; Bell, H. C.; Gustafson, J.; Warmington, J.; Wyllie, S. G. The mode of antimicrobial action of the essential oil of *Melaleuca alternifolia* (tea tree oil). *J. Appl. Microbiol.* **2000**, *88* (1), 170−175.
(7) MENDOZA-YEPES, M. J.; SANCHEZ-HIDALGO, L. E.; MAERTENS, G.; MARIN-INIESTA, F. INHIBITION OF *LISTERIA MONOCYTOGENES* AND OTHER BACTERIA BY A PLANT ESSENTIAL OIL (DMC) IN SPANISH SOFT CHEESE. *Journal of Food Safety* **1997**, *17* (1), 47−55.
(8) Cutter, C. N. Antimicrobial Effect of Herb Extracts against *Escherichia coli* O157:H7, *Listeria monocytogenes*, and *Salmonella typhimurium* Associated with Beef†. *Journal of Food Protection* **2000**, *63* (5), 601−607.
(9) Hartmans, K. J.; Diepenhorst, P.; Bakker, W.; Gorris, L. G. M. The use of carvone in agriculture: sprout suppression of potatoes and antifungal activity against potato tuber and other plant diseases. *Industrial Crops and Products* **1995**, *4* (1), 3−13.
(10) Atarés, L.; Chiralt, A. Essential oils as additives in biodegradable films and coatings for active food packaging. *Trends in Food Science & Technology* **2016**, *48*, 51−62.
(11) Ruiz-Navajas, Y.; Viuda-Martos, M.; Sendra, E.; Perez-Alvarez, J. A.; Fernández-López, J. In vitro antibacterial and antioxidant properties of chitosan edible films incorporated with *Thymus moroderi* or *Thymus piperella* essential oils. *Food Control* **2013**, *30* (2), 386−392.
(12) Karkanrood, M. V.; Homayouni Tabrizi, M.; Ardalan, T.; Soltani, M.; Khadem, F.; Nosrat, T.; Moeini, S. *Pistacia atlantica* fruit essential oil nanoemulsions (PAEO-NE), an effective antiangiogenic therapeutic and cell-dependent apoptosis inducer on A549 human lung cancer cells. *Inorganic and Nano-Metal Chemistry* **2022**, 1−11.
(13) Milia, E.; Bullitta, S. M.; Mastandrea, G.; Szotáková, B.; Schoubben, A.; Langhansová, L.; Quartu, M.; Bortone, A.; Eick, S. Leaves and fruits preparations of *Pistacia lentiscus* L.: a review on the ethnopharmacological uses and implications in inflammation and infection. *Antibiotics* **2021**, *10* (4), 425.
(14) Soulaidopoulos, S.; Tsiogka, A.; Chrysohoou, C.; Lazarou, E.; Aznaouridis, K.; Doundoulakis, I.; Tyrovola, D.; Tousoulis, D.; Tsioufis, K.; Vlachopoulos, C.; Lazaros, G. Overview of Chios Mastic Gum (*Pistacia lentiscus*) Effects on Human Health. *Nutrients* **2022**, *14* (3), 590.
(15) Pachi, V. K.; Mikropoulou, E. V.; Gkiouvetidis, P.; Siafakas, K.; Argyropoulou, A.; Angelis, A.; Mitakou, S.; Halabalaki, M. Traditional uses, phytochemistry and pharmacology of Chios mastic gum (*Pistacia lentiscus* var. *Chia*, Anacardiaceae): A review. *Journal of Ethnopharmacology* **2020**, *254*, No. 112485.
(16) Mahjoub, F.; Rezayat, K. A.; Yousefi, M.; Mohebbi, M.; Salari, R. *Pistacia atlantica* Desf. A review of its traditional uses, phytochemicals and pharmacology. *J. Med. Life* **2018**, *11* (3), 180.
(17) Ahmed, Z. B.; Yousfi, M.; Viaene, J.; Dejaegher, B.; Demeyer, K.; Vander Heyden, Y. Four *Pistacia atlantica* subspecies (*atlantica*, *cabulica*, *kurdica* and *mutica*): A review of their botany, ethnobotany, phytochemistry and pharmacology. *J. Ethnopharmacol.* **2021**, *265*, No. 113329.
(18) Ahmad, R.; Almubayedh, H.; Ahmad, N.; Naqvi, A. A.; Riaz, M. Ethnobotany, ethnopharmacology, phytochemistry, biological activities and toxicity of *Pistacia chinensis* subsp. integerrima: A comprehensive review. *Phytotherapy Research* **2020**, *34* (11), 2793−2819.
(19) Rauf, A.; Patel, S.; Uddin, G.; Siddiqui, B. S.; Ahmad, B.; Muhammad, N.; Mabkhot, Y. N.; Hadda, T. B. Phytochemical, ethnomedicinal uses and pharmacological profile of genus Pistacia. *Biomedicine & Pharmacotherapy* **2017**, *86*, 393−404.
(20) Kirollos, F.; Elhawary, S.; Salama, O.; Elkhawas, Y. LC-ESI-MS/MS and cytotoxic activity of three Pistacia species. *Natural Product Research* **2019**, *33* (12), 1747−1750.
(21) Serifi, I.; Tzima, E.; Bardouki, H.; Lampri, E.; Papamarcaki, T. Effects of the Essential Oil from *Pistacia lentiscus* Var. *chia* on the Lateral Line System and the Gene Expression Profile of Zebrafish (Danio rerio). *Molecules* **2019**, *24* (21), 3919.
(22) Huwez, F. U.; Thirlwell, D.; Cockayne, A.; Ala'Aldeen, D. A. A. Mastic Gum Kills *Helicobacter pylori*. *New England Journal of Medicine* **1998**, *339* (26), 1946−1946.
(23) Marone, P.; Bono, L.; Leone, E.; Bona, S.; Carretto, E.; Perversi, L. Bactericidal Activity of *Pistacia lentiscus* Mastic Gum Against *Helicobacter pylori*. *Journal of Chemotherapy* **2001**, *13* (6), 611−614.
(24) Kottakis, F.; Kouzi-Koliakou, K.; Pendas, S.; Kountouras, J.; Choli-Papadopoulou, T. Effects of mastic gum *Pistacia lentiscus* var. *Chia* on innate cellular immune effectors. *European Journal of Gastroenterology & Hepatology* **2009**, *21* (2), 143−149.
(25) Dabos, K. J.; Sfika, E.; Vlatta, L. J.; Giannikopoulos, G. The effect of mastic gum on *Helicobacter pylori*: A randomized pilot study. *Phytomedicine* **2010**, *17* (3), 296−299.
(26) HMPC Assessment report on *Pistacia lentiscus* L., resin (mastix); Science Medicines Health: European Medicines Agency, 7/7/2015, 2015; p 43.
(27) Tassou, C. C.; Nychas, G. J. E. Antimicrobial activity of the essential oil of mastic gum (*Pistacia lentiscus* var. *chia*) on Gram positive and Gram negative bacteria in broth and in Model Food System. *International Biodeterioration & Biodegradation* **1995**, *36* (3), 411−420.
(28) Aouinti, F.; Imelouane, B.; Tahri, M.; Wathelet, J. P.; Amhamdi, H.; Elbachiri, A. New study of the essential oil, mineral composition and antibacterial activity of *Pistacia lentiscus* L. from Eastern Morocco. *Res. Chem. Intermed.* **2014**, *40* (8), 2873−2886.
(29) Mezni, F.; Aouadhi, C.; Khouja, M. L.; Khaldi, A.; Maaroufi, A. In vitro antimicrobial activity of *Pistacia lentiscus* L. edible oil and phenolic extract. *Natural Product Research* **2015**, *29* (6), 565−570.
(30) Saiah, H.; Allem, R.; Kebir, F. Z. E. Antioxidant and antibacterial activities of six Algerian medicinal plants. *Int. J. Pharm. Pharm. Sci.* **2016**, *8*, 367−374.
(31) Mandrone, M.; Bonvicini, F.; Lianza, M.; Sanna, C.; Maxia, A.; Gentilomi, G. A.; Poli, F. Sardinian plants with antimicrobial potential. Biological screening with multivariate data treatment of thirty-six extracts. *Industrial Crops and Products* **2019**, *137*, 557−565.
(32) Milia, E.; Usai, M.; Szotáková, B.; Elstnerová, M.; Králová, V.; D'hallewin, G.; Spissu, Y.; Barberis, A.; Marchetti, M.; Bortone, A.; Campanella, V.; Mastandrea, G.; Langhansová, L.; Eick, S. The Pharmaceutical Ability of *Pistacia lentiscus* L. Leaves Essential Oil Against Periodontal Bacteria and Candida sp. and Its Anti-Inflammatory Potential. *Antibiotics* **2020**, *9* (6), 281.
(33) Iauk, L.; Ragusa, S.; Rapisarda, A.; Franco, S.; Nicolosi, V. M. In Vitro Antimicrobial Activity of *Pistacia lentiscus* L. Extracts: Preliminary Report. *Journal of Chemotherapy* **1996**, *8* (3), 207−209.
(34) Di Pierro, F.; Sagheddu, V.; Galletti, S.; Forti, M.; Elli, M.; Bertuccioli, A.; Gaeta, S. Antibacterial activity of a fractionated *Pistacia lentiscus* oil against pharyngeal and ear pathogens, alone or in combination with antibiotics. *Frontiers in Microbiology* **2021**, *12*, No. 686942.
(35) Fahmy, S. A.; Sedky, N. K.; Ramzy, A.; Abdelhady, M. M. M.; Alabrahim, O. A. A.; Shamma, S. N.; Azzazy, H. M. E.-S. Green extraction of essential oils from *Pistacia lentiscus* resins: Encapsulation into Niosomes showed improved preferential cytotoxic and apoptotic effects against breast and ovarian cancer cells. *Journal of Drug Delivery Science and Technology* **2023**, *87*, No. 104820.

https://doi.org/10.1021/acsomega.3c07413
ACS Omega 2024, 9, 12622−12634

(36) Gortzi, O.; Rovoli, M.; Katsoulis, K.; Graikou, K.; Karagkini, D.-A.; Stagos, D.; Kouretas, D.; Tsaknis, J.; Chinou, I. Study of stability, cytotoxic and antimicrobial activity of chios mastic gum fractions (neutral, acidic) after encapsulation in liposomes. *Foods* **2022**, *11* (3), 271.
(37) El-Chaghaby, G. A.; Ahmad, A. F. Biosynthesis of silver nanoparticles using *Pistacia lentiscus* leaves extract and investigation of their antimicrobial effect. *Orient. J. Chem.* **2011**, *27* (3), 929. http://www.orientjchem.org/?p=24402
(38) Vrouvaki, I.; Koutra, E.; Kornaros, M.; Avgoustakis, K.; Lamari, F. N.; Hatziantoniou, S. Polymeric nanoparticles of *Pistacia lentiscus* var. *chia* essential oil for cutaneous applications. *Pharmaceutics* **2020**, *12* (4), 353.
(39) Pinho, E.; Grootveld, M.; Soares, G.; Henriques, M. Cyclodextrin-based hydrogels toward improved wound dressings. *Critical Reviews in Biotechnology* **2014**, *34* (4), 328−337.
(40) Loftsson, T.; Duchêne, D. Cyclodextrins and their pharmaceutical applications. *Int. J. Pharm.* **2007**, *329* (1), 1−11.
(41) *CHMP Cyclodextrins used as excipients*; Science Medicines Health: European Medicines Agency, 9/10/2017, 2017; p 16.
(42) CHMP *Questions and answers on cyclodextrins used as excipients in medicinal products for human use*; Science Medicines Health: European Medicines Agency, 9/10/2017, 2017; p 9.
(43) Waleczek, K. J.; Marques, H. M. C.; Hempel, B.; Schmidt, P. C. Phase solubility studies of pure (−)-α-*bisabolol* and *camomile* essential oil with β-cyclodextrin. *Eur. J. Pharm. Biopharm.* **2003**, *55* (2), 247−251.
(44) Garnero, C.; Zoppi, A.; Genovese, D.; Longhi, M. Studies on trimethoprim:hydroxypropyl-β-cyclodextrin: aggregate and complex formation. *Carbohydr. Res.* **2010**, *345* (17), 2550−2556.
(45) Braga, S. S. Cyclodextrins: Emerging Medicines of the New Millennium. *Biomolecules* **2019**, *9* (12), 801.
(46) Becktel, D. A.; Zbesko, J. C.; Frye, J. B.; Chung, A. G.; Hayes, M.; Calderon, K.; Grover, J. W.; Li, A.; Garcia, F. G.; Tavera-Garcia, M. A.; Schnellmann, R. G.; Wu, H.-J. J.; Nguyen, T.-V. V.; Doyle, K. P. Repeated Administration of 2-Hydroxypropyl-β-Cyclodextrin (HPβCD) Attenuates the Chronic Inflammatory Response to Experimental Stroke. *J. Neurosci.* **2022**, *42* (2), 325−348.
(47) Zhang, G.; Yuan, C.; Sun, Y. Effect of Selective Encapsulation of Hydroxypropyl-β-cyclodextrin on Components and Antibacterial Properties of *Star Anise* Essential Oil. *Molecules* **2018**, *23* (5), 1126.
(48) Ciobanu, A.; Mallard, I.; Landy, D.; Brabie, G.; Nistor, D.; Fourmentin, S. Retention of aroma compounds from *Mentha piperita* essential oil by cyclodextrins and crosslinked cyclodextrin polymers. *Food Chem.* **2013**, *138* (1), 291−297.
(49) Kfoury, M.; Hădărugă, N. G.; Hădărugă, D. I.; Fourmentin, S., 4 - Cyclodextrins as encapsulation material for flavors and aroma. In *Encapsulations*; Grumezescu, A. M., Ed.; Academic Press: 2016; pp 127−192.
(50) Kfoury, M.; Auezova, L.; Greige-Gerges, H.; Fourmentin, S. Promising applications of cyclodextrins in food: Improvement of essential oils retention, controlled release and antiradical activity. *Carbohydr. Polym.* **2015**, *131*, 264−272.
(51) Liu, H.; Yang, G.; Tang, Y.; Cao, D.; Qi, T.; Qi, Y.; Fan, G. Physicochemical characterization and pharmacokinetics evaluation of β-caryophyllene/β-cyclodextrin inclusion complex. *Int. J. Pharm.* **2013**, *450* (1), 304−310.
(52) Tao, F.; Hill, L. E.; Peng, Y.; Gomes, C. L. Synthesis and characterization of β-cyclodextrin inclusion complexes of *thymol* and *thyme* oil for antimicrobial delivery applications. *LWT - Food Science and Technology* **2014**, *59* (1), 247−255.
(53) Rakmai, J.; Cheirsilp, B.; Mejuto, J. C.; Torrado-Agrasar, A.; Simal-Gándara, J. Physico-chemical characterization and evaluation of bio-efficacies of *black pepper* essential oil encapsulated in hydroxypropyl-beta-cyclodextrin. *Food Hydrocolloids* **2017**, *65*, 157−164.
(54) Kamimura, J. A.; Santos, E. H.; Hill, L. E.; Gomes, C. L. Antimicrobial and antioxidant activities of carvacrol microencapsulated in hydroxypropyl-beta-cyclodextrin. *LWT - Food Science and Technology* **2014**, *57* (2), 701−709.
(55) Bintsis, T. Foodborne pathogens. *AIMS Microbiol.* **2017**, *3* (3), 529−563.
(56) Bennik, M. H. J. PSEUDOMONAS | *Pseudomonas aeruginosa*. In *Encyclopedia of Food Microbiology*; Robinson, R. K., Ed.; Elsevier: Oxford, 1999; pp 1867−1871.
(57) Neves, P. R.; McCulloch, J. A.; Mamizuka, E. M.; Lincopan, N. PSEUDOMONAS | *Pseudomonas aeruginosa*. In *Encyclopedia of Food Microbiology*; 2nd ed.; Batt, C. A.; Tortorello, M. L., Eds.; Academic Press: Oxford, 2014; pp 253−260.
(58) Pachi, V. K.; Mikropoulou, E. V.; Dimou, S.; Dionysopoulou, M.; Argyropoulou, A.; Diallinas, G.; Halabalaki, M. Chemical Profiling of *Pistacia lentiscus* var. *Chia* Resin and Essential Oil: Ageing Markers and Antimicrobial Activity. *Processes* **2021**, *9* (3), 418.
(59) Tabanca, N.; Nalbantsoy, A.; Kendra, P. E.; Demirci, F.; Demirci, B. Chemical Characterization and Biological Activity of the Mastic Gum Essential Oils of *Pistacia lentiscus* var. *chia* from Turkey. *Molecules* **2020**, *25* (9), 2136.
(60) Azzazy, H. M. E.-S.; Abdelnaser, A.; Al Mulla, H.; Sawy, A. M.; Shamma, S. N.; Elhusseiny, M.; Alwahibi, S.; Mahdy, N. K.; Fahmy, S. A. Essential Oils Extracted from *Boswellia sacra* Oleo Gum Resin Loaded into PLGA−PCL Nanoparticles: Enhanced Cytotoxic and Apoptotic Effects against Breast Cancer Cells. *ACS Omega* **2023**, *8* (1), 1017−1025.
(61) Karathanos, V. T.; Mourtzinos, I.; Yannakopoulou, K.; Andrikopoulos, N. K. Study of the solubility, antioxidant activity and structure of inclusion complex of vanillin with β-cyclodextrin. *Food Chem.* **2007**, *101* (2), 652−658.
(62) Rakmai, J.; Cheirsilp, B.; Torrado-Agrasar, A.; Simal-Gándara, J.; Mejuto, J. C. Encapsulation of *yarrow* essential oil in hydroxypropyl-beta-cyclodextrin: physiochemical characterization and evaluation of bio-efficacies. *CyTA - Journal of Food* **2017**, *15* (3), 409−417.
(63) Hill, L. E.; Gomes, C.; Taylor, T. M. Characterization of beta-cyclodextrin inclusion complexes containing essential oils (*trans-cinnamaldehyde*, *eugenol*, *cinnamon bark*, and *clove bud* extracts) for antimicrobial delivery applications. *LWT - Food Science and Technology* **2013**, *51* (1), 86−93.
(64) Yuan, C.; Wang, Y.; Liu, Y.; Cui, B. Physicochemical characterization and antibacterial activity assessment of *lavender* essential oil encapsulated in hydroxypropyl-beta-cyclodextrin. *Industrial Crops and Products* **2019**, *130*, 104−110.
(65) Santos, E. H.; Kamimura, J. A.; Hill, L. E.; Gomes, C. L. Characterization of carvacrol beta-cyclodextrin inclusion complexes as delivery systems for antibacterial and antioxidant applications. *LWT - Food Science and Technology* **2015**, *60* (1), 583−592.
(66) Rakmai, J.; Cheirsilp, B.; Mejuto, J. C.; Simal-Gándara, J.; Torrado-Agrasar, A. Antioxidant and antimicrobial properties of encapsulated *guava* leaf oil in hydroxypropyl-beta-cyclodextrin. *Industrial Crops and Products* **2018**, *111*, 219−225.
(67) Orzali, L.; Valente, M. T.; Scala, V.; Loreti, S.; Pucci, N. Antibacterial Activity of Essential Oils and *Trametes versicolor* Extract against *Clavibacter michiganensis* subsp. *michiganensis* and *Ralstonia solanacearum* for Seed Treatment and Development of a Rapid In Vivo Assay. *Antibiotics* **2020**, *9* (9), 628.
(68) Rigling, M.; Fraatz, M. A.; Trögel, S.; Sun, J.; Zorn, H.; Zhang, Y. Aroma Investigation of Chios Mastic Gum (*Pistacia lentiscus* Variety *Chia*) Using Headspace Gas Chromatography Combined with Olfactory Detection and Chiral Analysis. *J. Agric. Food Chem.* **2019**, *67* (49), 13420−13429.
(69) Schachner-Nedherer, A.-L.; Werzer, O.; Zimmer, A. A Protocol To Characterize Peptide-Based Drug Delivery Systems for miRNAs. *ACS Omega* **2019**, *4* (4), 7014−7022.
(70) Wei, M.-X.; Liu, C.-H.; Lee, H.; Lee, B.-W.; Hsu, C.-H.; Lin, H.-P.; Wu, Y.-C. Synthesis of High-Performance Photonic Crystal Film for SERS Applications via Drop-Coating Method. *Coatings* **2020**, *10* (7), 679.
(71) Loftsson, T.; Másson, M.; Brewster, M. E. Self-Association of Cyclodextrins and Cyclodextrin Complexes. *J. Pharm. Sci.* **2004**, *93* (5), 1091−1099.

https://doi.org/10.1021/acsomega.3c07413
ACS Omega 2024, 9, 12622−12634

(72) Guimarães, A. G.; Oliveira, M. A.; Alves, R. d. S.; Menezes, P. d. P.; Serafini, M. R.; de Souza Araújo, A. A.; Bezerra, D. P.; Quintans Júnior, L. J. Encapsulation of carvacrol, a monoterpene present in the essential oil of *oregano*, with *β*-cyclodextrin, improves the pharmacological response on cancer pain experimental protocols. *Chemico-Biological Interactions* **2015**, *227*, 69−76.
(73) Marreto, R. N.; Almeida, E. E. C. V.; Alves, P. B.; Niculau, E. S.; Nunes, R. S.; Matos, C. R. S.; Araújo, A. A. S. Thermal analysis and gas chromatography coupled mass spectrometry analyses of hydroxypropyl-*β*-cyclodextrin inclusion complex containing *Lippia gracilis* essential oil. *Thermochim. Acta* **2008**, *475* (1), 53−58.
(74) Seo, E.-J.; Min, S.-G.; Choi, M.-J. Release characteristics of freeze-dried *eugenol* encapsulated with *β*-cyclodextrin by molecular inclusion method. *J. Microencapsulation* **2010**, *27* (6), 496−505.
(75) Choi, M.-J.; Soottitantawat, A.; Nuchuchua, O.; Min, S.-G.; Ruktanonchai, U. Physical and light oxidative properties of *eugenol* encapsulated by molecular inclusion and emulsion−diffusion method. *Food Research International* **2009**, *42* (1), 148−156.
(76) Aksamija, A.; Polidori, A.; Plasson, R.; Dangles, O.; Tomao, V. The inclusion complex of rosmarinic acid into beta-cyclodextrin: A thermodynamic and structural analysis by NMR and capillary electrophoresis. *Food Chem.* **2016**, *208*, 258−263.
(77) Gao, B.; Wang, G.; Li, B.; Wu, L. Self-Inclusion and Dissociation of a Bridging *β*-Cyclodextrin Triplet. *ACS Omega* **2020**, *5* (14), 8127−8136.
(78) Rodríguez-López, M. I.; Mercader-Ros, M. T.; Lucas-Abellán, C.; Pellicer, J. A.; Pérez-Garrido, A.; Pérez-Sánchez, H.; Yáñez-Gascón, M. J.; Gabaldón, J. A.; Núñez-Delicado, E. Comprehensive Characterization of Linalool-HP-*β*-Cyclodextrin Inclusion Complexes. *Molecules* **2020**, *25* (21), 5069.
(79) Saha, S.; Roy, A.; Roy, K.; Roy, M. N. Study to explore the mechanism to form inclusion complexes of *β*-cyclodextrin with vitamin molecules. *Sci. Rep.* **2016**, *6* (1), 35764.
(80) Rodríguez-López, M. I.; Mercader-Ros, M. T.; López-Miranda, S.; Pellicer, J. A.; Pérez-Garrido, A.; Pérez-Sánchez, H.; Núñez-Delicado, E.; Gabaldón, J. A. Thorough characterization and stability of HP-*β*-cyclodextrin *thymol* inclusion complexes prepared by microwave technology: A required approach to a successful application in food industry. *Journal of the Science of Food and Agriculture* **2019**, *99* (3), 1322−1333.
(81) Khan, N.; Singh, A. K.; Saneja, A. Preparation, Characterization, and Antioxidant Activity of L-Ascorbic Acid/HP-β-Cyclodextrin Inclusion Complex-Incorporated Electrospun Nanofibers. *Foods* **2023**, *12* (7), 1363.
(82) Jiang, S.; Zhao, T.; Wei, Y.; Cao, Z.; Xu, Y.; Wei, J.; Xu, F.; Wang, H.; Shao, X. Preparation and characterization of *tea tree* oil/hydroxypropyl-*β*-cyclodextrin inclusion complex and its application to control brown rot in peach fruit. *Food Hydrocolloids* **2021**, *121*, No. 107037.
(83) Yuan, C.; Jin, Z.; Li, X. Evaluation of complex forming ability of hydroxypropyl-*β*-cyclodextrins. *Food Chem.* **2008**, *106* (1), 50−55.
(84) Chrysouli, M. P.; Banti, C. N.; Kourkoumelis, N.; Moushi, E. E.; Tasiopoulos, A. J.; Douvalis, A.; Papachristodoulou, C.; Hatzidimitriou, A. G.; Bakas, T.; Hadjikakou, S. K. Ciprofloxacin conjugated to diphenyltin(iv): a novel formulation with enhanced antimicrobial activity. *Dalton Transactions* **2020**, *49* (33), 11522−11535.
(85) Dhar, P.; Chan, P.; Cohen, D. T.; Khawam, F.; Gibbons, S.; Snyder-Leiby, T.; Dickstein, E.; Rai, P. K.; Watal, G. Synthesis, Antimicrobial Evaluation, and Structure−Activity Relationship of *α*-Pinene Derivatives. *J. Agric. Food Chem.* **2014**, *62* (16), 3548−3552.
(86) Rivas da Silva, A. C.; Lopes, P. M.; Barros de Azevedo, M. M.; Costa, D. C. M.; Alviano, C. S.; Alviano, D. S. Biological activities of *α*-pinene and *β*-pinene enantiomers. *Molecules* **2012**, *17* (6), 6305−6316.
(87) de Sousa Eduardo, L.; Farias, T. C.; Ferreira, S. B.; Ferreira, P. B.; Lima, Z. N.; Ferreira, S. B. Antibacterial activity and time-kill kinetics of positive enantiomer of *α*-pinene against strains of *Staphylococcus aureus* and *Escherichia coli*. *Current Topics in Medicinal Chemistry* **2018**, *18* (11), 917−924.
(88) Wang, T.; Li, B.; Si, H.; Lin, L.; Chen, L. Release characteristics and antibacterial activity of solid state *eugenol*/*β*-cyclodextrin inclusion complex. *Journal of Inclusion Phenomena and Macrocyclic Chemistry* **2011**, *71* (1), 207−213.

https://doi.org/10.1021/acsomega.3c07413
ACS Omega 2024, 9, 12622−12634